

OPEN

Retina Publish Ahead of Print

DOI: 10.1097/IAE.0000000000003957

Use of Hand-Held Optical Coherence Tomography during Retinopathy of Prematurity (ROP) Screening demonstrates an increased Outer Retina from early Postmenstrual Age in Preterm Infants with ROP.

Authors: Samira Anwar (FRCOphth)^{1,3*, \$}, Mintu Nath (PhD)^{2, \$}, Aarti Patel (MBChB.)¹, Straton Tyradellis (MD)³, Irene Gottlob (MD)^{1*} and Frank A Proudlock (PhD)^{1*}

Abbreviated title: *Increased Outer Retina noted in ROP*

Authors Affiliations

¹University of Leicester Ulverscroft Eye Unit, Robert Kilpatrick Clinical Sciences Building Leicester Royal Infirmary, Leicester, LE2 7LX, United Kingdom.

²Institute of Applied Health Sciences, Polwarth Building, The University of Aberdeen, Aberdeen, AB25 2ZD, United Kingdom.

³Department of Ophthalmology, University Hospitals of Leicester NHS Trust, Infirmary Square, LE1 5WW, Leicester, United Kingdom.

This is an open-access article distributed under the terms of the Creative Commons Attribution-Non Commercial-No Derivatives License 4.0 (CCBY-NC-ND), where it is permissible to download and share the work provided it is properly cited. The work cannot be changed in any way or used commercially without permission from the journal.

\$S Anwar and M Nath are joint first authors.

Study performed at the University Hospitals of Leicester NHS Trust and The University of Leicester.

Financial Support: Medical Research Council, London, UK (grant number: MR/N004566/1 and MR/J004189/1), Ulverscroft Foundation, Leicester, UK, Nystagmus Network UK.

Conflict of interest: No conflicting relationship exists for any author

Corresponding Author: S Anwar sa897@leicester.ac.uk

University of Leicester Ulverscroft Eye Unit, Robert Kilpatrick Clinical Sciences Building
Leicester Royal Infirmary, Leicester, LE1 5WW, United Kingdom.

Manuscript word count: (3000)

UNCORRECTED PROOF

Key Words

Retinal layers

Parafovea, fovea

Hand-held Optical Coherence Tomography

Prematurity, Preterm Infant

Retinopathy of Prematurity

Summary

Hand-held optical coherence tomography (HH-OCT) demonstrates increased foveal and parafoveal outer retina and reduced inner nuclear layer with retinopathy of prematurity (ROP) compared to no ROP in prematurity. There is future potential in developing a novel imaging biomarker for HH-OCT use during ROP screening.

Count 44 words

UNCORRECTED PROOF

Abstract

Purpose: To identify structural markers of active retinopathy of prematurity (ROP) in foveal and parafoveal retinal layers using hand-held optical coherence tomography (HH-OCT).

Methods: We acquired HH-OCT images (n=278) from a prospective mixed cross-sectional longitudinal observational study of 87 participants (23-36 weeks gestational age (GA); n=30 with ROP, n=57 without ROP) between 31 to 44 weeks postmenstrual age (PMA) excluding treated ROP and features of cystoid macular edema (CME). Six retinal layer thicknesses from the fovea to the parafovea were analysed at five locations up to 1000 μm temporally and nasally.

Results: The mean outer retinal thickness (OUTRETL) during active ROP increased at the fovea and parafovea from PMA 33 to 39 weeks ($p<0.001$) while the parafoveal inner nuclear layer (INL) and retinal nerve fiber layer (RNFL) reduced ($p<0.001$). OUTRETL at the fovea from 33 to 39 weeks PMA was consistently thicker in infants with ROP across all levels of prematurity (GA).

Conclusions: Increased foveal and parafoveal outer retina measured using HH-OCT shows potential as a marker for ROP screening.

Count: 170 words

Introduction

Retinopathy of prematurity (ROP), associated with preterm birth, shows changes of foveal and macular structure during the neonatal period as demonstrated using hand held optical coherence tomography (HH-OCT) during ROP screening.¹⁻⁵ Preterms also have persistence of foveal inner retinal layers, increased central foveal thickness (CFT) and outer layer delays.⁶⁻⁹ Additionally, inner nuclear layer (INL) intraretinal cystic spaces described as cystoid macular edema (CME) distort retinal structure and are present in up to 72% of preterm infants imaged before 42 weeks postmenstrual age (PMA).^{1,2,4,5,10,11}

Emerging preterm OCT studies suggest ROP influence is distinct from that of prematurity on foveal and parafoveal structure,^{10,12} and severity of prematurity is important in preterm retinal structure assessment.^{12,13}

Due to the limitations for objective quantitative measurement of infant retinal structure, efforts to determine consistent structural markers have been explored using HH-OCT to distinguish characteristics in preterms infants with ROP during screening.^{12,14}

Our aim was to assess ROP impact on individual foveal and parafoveal retinal layers using HH-OCT. We hypothesized that this would reveal pathologic structural changes related to ROP rather than prematurity. Demonstrating these differences opens future possibilities into identifying additional criteria that could be used during ROP screening and directing earlier treatment intervention in high-risk infants.

Methods

This was a prospective observational study completed between 2012 and 2015 in Leicester, United Kingdom, conducted under the tenets of the Declaration of Helsinki with approval by

a Local Ethics Committee (NRES committee, Nottingham East Midlands, United Kingdom). Patients were recruited from the Leicester Royal Infirmary neonatal and maternity unit, United Kingdom and all preterm babies from 31 to 44 weeks PMA who required ROP screening were eligible for inclusion in the study. An abnormal ocular examination other than diagnosis of ROP, treated ROP, and ROP stages 4 or 5 were exclusion criteria. For screening and imaging, ROP was defined as stages 1-3 using the UK guidelines¹⁵ and eyes were dilated using Cyclomydril® eye drops.

Imaging was performed from 31 to 44 weeks PMA at 1 to 2 weekly intervals using HH-OCT (Envisu C-Class, Leica Microsystems, Wetzlar, Germany) scan sequence consisting of 500 A scans and 100 B scans covering a rectangular volume of 5.0 mm x 10.0 x 2.0 mm. Further details can be found in supplemental digital content 1 (SDC1).

Retinal layer analysis

Analysis of HH-OCT images was performed using customized layer segmentation macros written in ImageJ software (United States National Institutes of Health, Bethesda, MD, <https://imagej.nih.gov/ij/>, downloaded in December 2013).

Scans were optimized for obtaining a single high-quality scan at the central retina and the lateral distance settings were corrected to account for the smaller axial lengths in the infant population using a conversion table according to PMA and GA from the data presented by Maldonado and colleagues.¹⁶

Foveal B-scans were flattened using the Bruch's membrane as a reference line and translating individual A-scans vertically. Boundary detection of the internal limiting membrane (ILM) was performed automatically using the ABSnake plugin

(http://imagejdocu.tudor.lu/doku.php?id=plugin:segmentation:active_contour:start). Manual fine adjustment of the fitted line was used to generate the final segmentation.

Other retinal layer borders were manually segmented using semi-automatic with manual correction techniques and definitions from previously reported literature.^{8,9,17-19} Individual layer thicknesses were calculated between border edges based on previous literature.^{20,21}

Details are shown in **Table 1**. Inner retinal layers were generally present across the central retina from 30 weeks' PMA using HH SD-OCT as previously reported.⁷⁻⁹ The external limiting membrane (ELM) was often absent in early gestational age (GA) compared with later GA, limiting segmentation of the outer retina. Therefore, the combined outer retina was defined from the lower margin of the inner nuclear layer (INL) to the upper margin of the retinal pigment epithelium (RPE) and labelled as OUTRETL.

Duplicate images were discarded. Images with intraretinal hypo-reflected spaces distorting the macula within the INL were defined as CME and manually separated from those where CME was absent in accordance with peer reviewed literature.¹⁰ Due to the disruption to retinal structure from CME, images showing CME present in one or both eyes were excluded from the study.

Locations 1000 μ m and 500 μ m nasal and temporal to the central fovea were chosen to be within the parafovea and foveal zone from histological studies of the developing eye.²²

Locations were measured from points taken on either side of the fovea up to 1000 μ m nasally and temporally.

Statistical Analysis

We fitted an additive mixed model to analyse the retinal thickness data on six retinal layers: retinal nerve fibre layer (RNFL), ganglion cell layer (GCL), inner plexiform layer (IPL), INL,

OUTRETL and the RPE. The model predictor variables included GA, PMA, location and ROP status (presence and absence).

The model also considered the two-way interaction terms of GA (and PMA) with location, and GA with ROP. Since the two-way interaction terms were significant ($p < 0.05$), we also considered three-way interaction terms with each retinal layer. To capture the non-linear shape of the retinal thickness in the entire nasal to temporal locations, the model incorporated the smoothing terms of the location by retinal layers, and location by ROP status. The smoothing term assumed the basis function as a Gaussian process model with 10 knots. To account for the multiple measurements on the same infant, we incorporated the random intercept of infant assuming an equal correlation between the measurements on the same infant. We also incorporated the fixed effect of the eye to compare the left and right eyes. However, the final model excluded the eye as a predictor variable as it was not statistically significant. The model allowed for a participant to be ROP-positive and ROP-negative at different time points. An individual was considered ROP-positive when the ROP was detected in at least one eye.

The validity of the basis dimension was assessed using visual methods and the k-index, and model assumptions were checked using appropriate residual plots. Since the pattern of the residuals resembles that of a normal distribution with heavier tails, we considered the residual distribution using the scaled-t family for heavy-tailed data. We obtained and compared the predicted means for ROP for pre-specified values of GA, PMA and location, and the p-values for the comparisons were obtained after employing Bonferroni correction so that the overall type 1 error is less than 0.05. The additive mixed model was fitted using the R package mgcv (version 1.8.24) and all statistical analyses were conducted in R.

Results

There were 112 preterm infants aged between 23 to 36 weeks GA of which 25 demonstrated CME and excluded, leaving 87 participants and 278 images for analysis. No infant had undergone any treatment for ROP. The number of infants according to GA was as follows: 12 \leq 24 weeks GA, 26 from 25 to 27 weeks GA, 29 from 28 to 29 weeks GA and 20 \geq 30 weeks GA. **Table 2** shows participant and image demographics according to ROP. **Table 3** presents the summary statistics on preterm infants included in the study.

Changes in foveal and parafoveal retinal layers associated with retinopathy of prematurity as the retina develops (increasing postmenstrual age 33 to 39 weeks)

We explored the differences in foveal and parafoveal architecture associated with the presence of ROP and non-ROP for individual layers at five locations and for three time points (PMA 33, 36, 39 weeks).

Figure 1 summarizes the changes associated with ROP in each of the foveal / parafoveal retinal segmented layers, at (A) 33 weeks, (B) 36 weeks, and (C) 39 weeks PMA at the fovea and 1000 μm and 500 μm temporally and nasally, using mean GA (27.5 weeks). **Table 4** reports the mean difference in retinal thickness between the presence and absence of ROP for each layer along with 95% confidence intervals and the adjusted p -values (Bonferroni adjustment).

Our analysis found the OUTRETL was significantly thicker during active ROP compared with non-ROP across timepoints PMA 33, 36 and 39 weeks at mean GA 27.5 weeks (see

Figure 1; Table 4 sections A, B and C). This was noted across the fovea and parafovea from 1000 μm nasally to 1000 μm temporally.

There was also a reduction in mean INL thickness for infants with active ROP compared with non-ROP measured in the temporal and nasal parafovea at PMA 33 weeks. By late PMA 39 weeks this reduction included the fovea.

At 33 weeks PMA, RNFL and RPE thickness reduced at the parafovea, but the mean thickness difference was not statistically significant ($p>0.05$) between ROP and non-ROP at PMA 36 and 39 weeks.

Supplementary Video 1 (SDC2) demonstrates the dynamic mean retinal thickness changes at mean GA (27.5 weeks) with PMA from 33 to 39 weeks between ROP and non-ROP infants for the RNFL, GCL, IPL, INL, OUTRETL and RPE. ROP is marked in red, non-ROP is marked in blue. The locations are marked as nasal (parafovea -1000 μ m and -500 μ m) and temporal (parafovea 1000 μ m and 500 μ m) and the fovea (0).

Changes in foveal and parafoveal layers associated with retinopathy of prematurity investigating degree of prematurity (gestational ages 24, 27.5, 30 weeks) as the retina develops (postmenstrual ages 33, 36 and 39 weeks).

Since we found significant differences between retinal layers for ROP at 33 to 39 weeks PMA using mean GA, we wanted to see if degree of prematurity also had an effect on the retinal layers. **Figure 2** summarizes the changes associated with ROP for various GA (24, 27.5 and 30 weeks) at 33-, 36- and 39-weeks PMA in each of the segmented retinal layers.

Tables 5, 6 and 7 (SDC3, SDC4 and SDC5 respectively) report the mean difference in retinal thickness between the presence and absence of ROP along with 95% confidence intervals and adjusted p -values (Bonferroni adjustment) at (A) 24 weeks, (B) 27 weeks and (C) 30 weeks GA at the five locations for PMA of 33, 36 and 39 weeks.

At 33 weeks PMA the OUTRETL consistently remained thicker at the fovea and at 500 μ m nasal and temporal to the fovea for all GA. We also found thicker GCL and IPL in extreme preterm infants (GA 24 weeks) with ROP compared with the non-ROP group across all locations. Conversely in preterm infants of GA 30 weeks with ROP, this pattern reversed with thinner GCL and IPL (see **Figure 2** GA 24 and GA 30 weeks).

When investigating the retinal layers at later time points (PMA 36 and 39 weeks) for 24-, 27- and 30-weeks GA, the OUTRETL was still greater in active ROP compared with non-ROP. The increased OUTRETL was greater for 30 weeks GA compared with 24 weeks GA for both ROP and non-ROP (see **Figure 2**; Tables 6 and 7 **SDC4** and **SDC5** respectively).

Examining the effect of location on retinal layers with GA, at the fovea the INL increased with severity of prematurity (see **Figure 2** GA 24 weeks compared with GA 30 weeks fovea, INL). However, GCL and IPL were reduced at the fovea in 24 weeks GA compared with 30 weeks GA in non-ROP, whereas both increased at the fovea in GA 24 weeks compared with 30 weeks GA in ROP.

Discussion

As the retina develops from early to late PMA (33 to 39 weeks), the preterm outer retina is significantly thicker at the fovea and parafovea for GA 30 weeks, and least for GA 24 weeks. This would concur with the delays reported in outer retinal development for extreme prematurity.⁶ However, when ROP was present, the outer retina was increased further for all gestational ages.

We found increased foveal and parafoveal INL at 24 weeks GA compared with 30 weeks GA. This is in keeping with other reports suggesting an effect on the foveal depth and

thickness from severity of prematurity.^{12,13} Examining the additional effect of ROP, at GA 27 and 30 weeks, INL thickness measured less when compared with non-ROP.

This was not found for 24 weeks GA, where the INL was even greater suggesting that ROP was an additional significant factor perhaps depending on stage of ROP, since the risk of ROP is greatest in extreme prematurity. However, we did not have enough infants in stages 1-3 or plus disease for the various GA to investigate this further (see **Table 2**) and could not exclude sub-clinical CME.

In the absence of ROP, the GCL and IPL reduced at the fovea more for 24 weeks GA compared with 30 weeks GA reflecting degree of prematurity. When exploring the presence of ROP, this pattern reversed, with earlier born infants measuring a thicker mean GCL and IPL at the fovea compared with later born infants. Our findings are in agreement with Mangalesh et al¹⁰ that ROP plays a role in addition to severity of prematurity in retinal development with PMA when measured till 42 weeks PMA. However, we have also shown that dynamic changes occur from early to late PMA with ROP and GA.

ROP and increased outer retinal layers

Reduced outer retina at the fovea relates to severity of prematurity where the photoreceptors are delayed during development⁶ but few studies have separated active untreated ROP from prematurity in the analysis of individual retinal layer structure and measurements using HH-OCT during the developing postnatal period.¹⁰ In a large study by O Sullivan and colleagues¹³ the authors concluded that more premature infants had thicker foveal outer retinal layers. Out of 204 eyes, 26 were treated and the impact of ROP was unclear on outer retinal analysis. In contrast, we specifically wished to understand the impact of ROP and GA in multivariate analyses and excluded treated infants. We found that ROP influences the outer

retina, with increased thickness in preterm infants with ROP since ROP risk is greatest in very preterm born babies. We suggest that our findings are in accordance with O Sullivan et al but in addition we have delineated the processes that can affect foveal outer layers with respect to ROP as well as GA.

In ROP pathogenesis, the photoreceptor outer layers are metabolically active driving oxygen requirement. Image acquisition prior to 32 weeks PMA was not possible so it is unclear if infants developed greater outer retina thickness and were more at risk of developing ROP, or if the increased outer retina developed in the presence of active ROP. However, the outer retina in preterm infants without ROP measured less compared with ROP suggesting that outer retinal layer increase is associated with ROP presence. Possibly, this increase results from factors released due to either parafoveal or peripheral retinal ischemia or other unknown mechanism.

Reduction of inner nuclear layer during ROP

We hypothesized that HH-OCT of retinal structure during ROP may reveal surrogate markers of changes distinct from prematurity and that the INL reduction in our study could represent ischaemia reflecting ROP presence.

In adults, paracentral maculopathy due to small retinal vessel intermediate and deep vascular plexus ischemia has been described in association with several vascular retinopathies and identified by characteristic lesions found using spectral domain OCT (SD-OCT).²³ The location of the lesions is described to be in either the INL or below the OPL.^{24,25} However, in developing preterm infants, the outer retina is immature and the OPL is either poorly visualized or absent on imaging.

The deep vascular networks are located above and below the INL, while the intermediate capillary plexus component is located at the INL and IPL interface.^{26,27} The INL contains the bodies of Müller cells which express vascular endothelial growth factor (VEGF) and are known to respond to photoreceptor injury or stress.²⁸ Retinal ischemia, as seen in oxygen-induced retinopathy (OIR) in rats, increases Müller cell expression of VEGF type A²⁹ and in a vascular/avascular retinal OIR mouse model, decreased inner retinal thickness was associated with reduced capillary density and the development of large vessel tortuosity.³⁰ The reduction in INL in our study may have been found in comparison to an abnormal increase in INL due to sub-clinical CME in our images. Preterm infant CME has been observed primarily in the INL.¹¹ We did not calculate a predictor measure for INL for the exclusion of CME as we did not have sufficient data to do this using a ROC curve¹³ however our analysis was powered for ROP and individual layers, and applied equally to both groups (with and without ROP). Images with CME were identified in our study accordance with peer reviewed literature^{2,7,10} and specifically excluded.

We also found increased INL related to increased severity of prematurity as reported by O'Sullivan and colleagues¹³ but in our study, additionally, the INL was reduced in ROP compared with non-ROP, suggesting ROP is a factor in this change rather than prematurity alone for the infants with ROP.

Limitations

There is paucity of information regarding the developing preterm retinal vasculature and structural disparities found using HH-OCT could represent unrelated vascular characteristics between the two groups. Perifoveal vascular development, especially the deep vascular complex, may not have been fully developed at the time of imaging between 33- and 39-

weeks PMA. While it is possible that additional delays to this network developing due to ROP may reflect HH-OCT findings, the suggestion of retinal ischemia and reduced INL remains speculative.

O'Sullivan et al¹³ calculated a threshold INL thickness as a surrogate measure in order to distinguish between CME and non-CME therefore reducing the possibility of contamination in retinal layer measurements. Our segmentation and analysis algorithm differs and we did not have enough CME data to define our criteria in the same way. Furthermore, as the resolution of portable OCT improves there will be less subjectivity in subclinical CME detection, offering further insight. Including more infants with earlier GA and ROP stages 1 to 3 in order to investigate a dose response between ROP severity and the OUTREL would strengthen the study conclusions.

Conclusions

Our study demonstrates the dynamic differences between PMA, prematurity and ROP on foveal and parafoveal development. Extreme prematurity demonstrates a differential between ROP and non ROP foveal INL. When the effects of ROP were examined with extreme prematurity, we found reduced INL and increased outer retina, acknowledging that subclinical CME could still be present within the INL. Although ROP severity could not be characterised, we believe our study presents possibilities that merit further investigation.

SDC1 Methodology -<http://links.lww.com/IAE/C82>

SDC2 video 1 -<http://links.lww.com/IAE/C83>

SDC3 Table 5 -<http://links.lww.com/IAE/C84>

SDC4 Table 6 -<http://links.lww.com/IAE/C85>

SDC5 Table 7 -<http://links.lww.com/IAE/C86>

References

1. Gursoy H., Bilgeç M. D., Erol N et al. *The macular findings on spectral-domain optical coherence tomography in premature infants with or without retinopathy of prematurity*. Int Ophthalmol, 2016. **36**(4): p. 591-600.
2. Vinekar A., Avadhani K., Sivakumar M., et al. *Understanding clinically undetected macular changes in early retinopathy of prematurity on spectral domain optical coherence tomography*. Invest Ophthalmol Vis Sci, 2011. **52**(8): p. 5183-8.
3. Lee A.C., Maldonado R.S., Sarin N., et al. *Macular features from spectral-domain optical coherence tomography as an adjunct to indirect ophthalmoscopy in retinopathy of prematurity*. Retina, 2011. **31**(8): p. 1470-82.
4. Dubis A.M., Subramaniam C.D., Godara P., et al. *Subclinical macular findings in infants screened for retinopathy of prematurity with spectral-domain optical coherence tomography*. Ophthalmology, 2013. **120**(8): p. 1665-71.
5. Erol M.K., Ozdemir O., Coban D. T., et al. *Macular findings obtained by spectral domain optical coherence tomography in retinopathy of prematurity*. J Ophthalmol, 2014. **2014**: p. 468653.
6. Vajzovic L., Rothman A. L., Tran-Viet D., et al. *Delay in retinal photoreceptor development in very preterm compared to term infants*. Invest Ophthalmol Vis Sci, 2015. **56**(2): p. 908-13.
7. Maldonado R.S., O'Connell R. V., Sarin N., et al. *Dynamics of human foveal development after premature birth*. Ophthalmology, 2011. **118**(12): p. 2315-25.
8. Dubis A.M., Costakos D. M., Subramaniam C. D., et al. *Evaluation of Normal Human Foveal Development using Optical Coherence Tomography and Histologic Examination*. Arch Ophthalmol, 2012. **130**(10): p. 1291-1300.

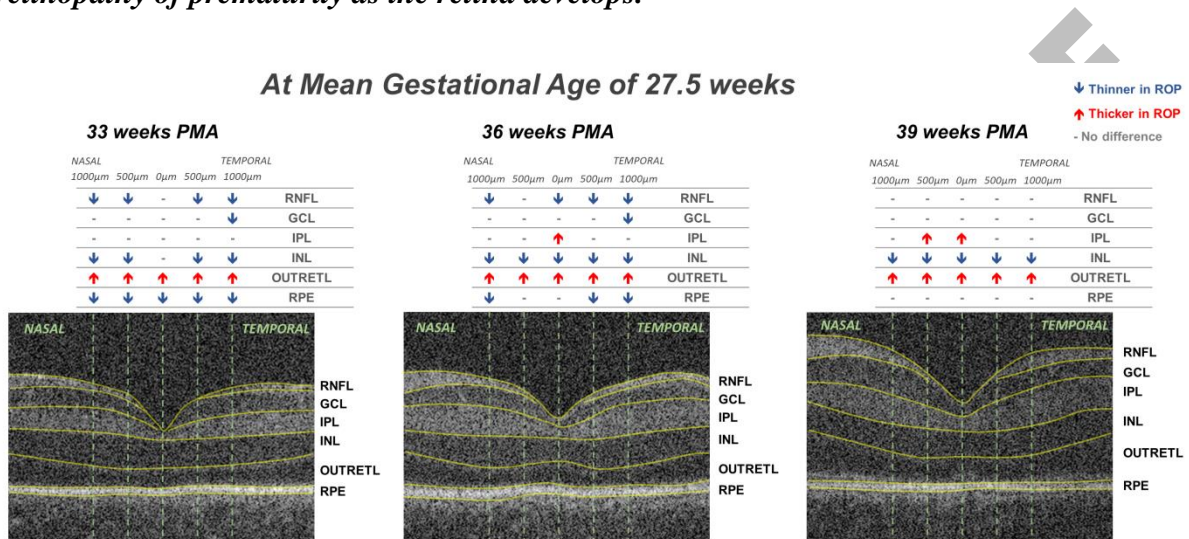
9. Vajzovic L., Hendrickson A. E., O'Connell R. V., et al. *Maturation of the human fovea: correlation of spectral-domain optical coherence tomography findings with histology*. Am. J. Ophthalmol., 2012. **154**(5): p. 779-789 e2.
10. Mangalesh S., McGeehan B., Tai V., et al. *Macular OCT Characteristics at 36 Weeks' Postmenstrual Age in Infants Examined for Retinopathy of Prematurity*. Ophthalmol Retina, 2020.
11. Maldonado R.S., O'Connell R., Ascher S. B., et al. *Spectral-domain optical coherence tomographic assessment of severity of cystoid macular edema in retinopathy of prematurity*. Arch Ophthalmol, 2012. **130**(5): p. 569-78.
12. Anwar S., Nath M., Patel A., et al. *Potential Utility of Foveal Morphology in Preterm Infants Measured Using Hand-Held Optical Coherence Tomography in Retinopathy of Prematurity Screening*. Retina, 2019.
13. O'Sullivan M.L., Ying G-S., Mangalesh S., et al. *Foveal Differentiation and Inner Retinal Displacement Are Arrested in Extremely Premature Infants*. Invest Ophthalmol Vis Sci, 2021. **62**(2): p. 25.
14. Maldonado R.S., Yuan E., Tran-Viet D., et al. *Three-dimensional assessment of vascular and perivascular characteristics in subjects with retinopathy of prematurity*. Ophthalmology, 2014. **121**(6): p. 1289-96.
15. RCOphth, RCPCH, and BAPM & BLISS. *Guideline for the Screening and Treatment of Retinopathy of Prematurity 2008*: United Kingdom.
16. Maldonado R.S., Izatt J. A., Sarin N., et al. *Optimizing hand-held spectral domain optical coherence tomography imaging for neonates, infants, and children*. Invest Ophthalmol Vis Sci, 2010. **51**(5): p. 2678-85.

17. Srinivasan V.J., Monson B. K., Wojtkowski M., et al. *Characterization of outer retinal morphology with high-speed, ultrahigh-resolution optical coherence tomography*. Invest Ophthalmol Vis Sci, 2008. **49**(4): p. 1571-9.
18. Spaide, R.F. and C.A. Curcio. *Anatomical correlates to the bands seen in the outer retina by optical coherence tomography. Literature Review and Model*. Retina., 2011. **31**(8): p. 1609-1619.
19. Staurenghi G., Sadda S., Chakravarthy U., et al. *Proposed lexicon for anatomic landmarks in normal posterior segment spectral-domain optical coherence tomography: the IN*OCT consensus*. Ophthalmology, 2014. **121**(8): p. 1572-8.
20. Bagci A.M., Shahidi M., Ansari R., et al. *Thickness profiles of retinal layers by optical coherence tomography image segmentation*. Am J Ophthalmol, 2008. **146**(5): p. 679-87.
21. Loduca A.L., Zhang C., Zelkha R., and Shahidi M. *Thickness mapping of retinal layers by spectral-domain optical coherence tomography*. Am J Ophthalmol, 2010. **150**(6): p. 849-55.
22. Hendrickson A.E. and C. Yuodelis. *The Morphological Development of the Human Fovea*. Ophthalmology, 1984. **91**(6): p. 603-612.
23. Chen X., Rahimy E., Sergott R. C., et al. *Spectrum of Retinal Vascular Diseases Associated With Paracentral Acute Middle Maculopathy*. Am J Ophthalmol, 2015. **160**(1): p. 26-34 e1.
24. Sarraf D., Rahimy E., Fawzi A. A., et al. *Paracentral acute middle maculopathy: a new variant of acute macular neuroretinopathy associated with retinal capillary ischemia*. JAMA Ophthalmol, 2013. **131**(10): p. 1275-87.

25. Sridhar J., Shahlaee A., Rahimy E., et al. *Optical Coherence Tomography Angiography and En Face Optical Coherence Tomography Features of Paracentral Acute Middle Maculopathy*. Am J Ophthalmol, 2015. **160**(6): p. 1259-1268 e2.
26. Campbell J.P., Nudleman E., Yang J., et al. *Handheld Optical Coherence Tomography Angiography and Ultra-Wide-Field Optical Coherence Tomography in Retinopathy of Prematurity*. JAMA Ophthalmol, 2017. **135**(9): p. 977-981.
27. Provis J.M. *Development of the Primate Retinal Vasculature*. Prog. Ret. Eye Res., 2001. **20**(6): p. 799-821.
28. Goldman D. *Muller glial cell reprogramming and retina regeneration*. Nat Rev Neurosci, 2014. **15**(7): p. 431-42.
29. Becker S., Wang H., Simmons A. B., et al. *Targeted Knockdown of Overexpressed VEGFA or VEGF164 in Muller cells maintains retinal function by triggering different signaling mechanisms*. Sci Rep, 2018. **8**(1): p. 2003.
30. Mezu-Ndubuisi O.J., Adams T., Taylor L. K., et al. *Simultaneous assessment of aberrant retinal vascularization, thickness, and function in an in vivo mouse oxygen-induced retinopathy model*. Eye (Lond), 2018.

Figure Legends

Figure 1. A summary of changes in foveal / parafoveal retinal layers associated with retinopathy of prematurity as the retina develops.

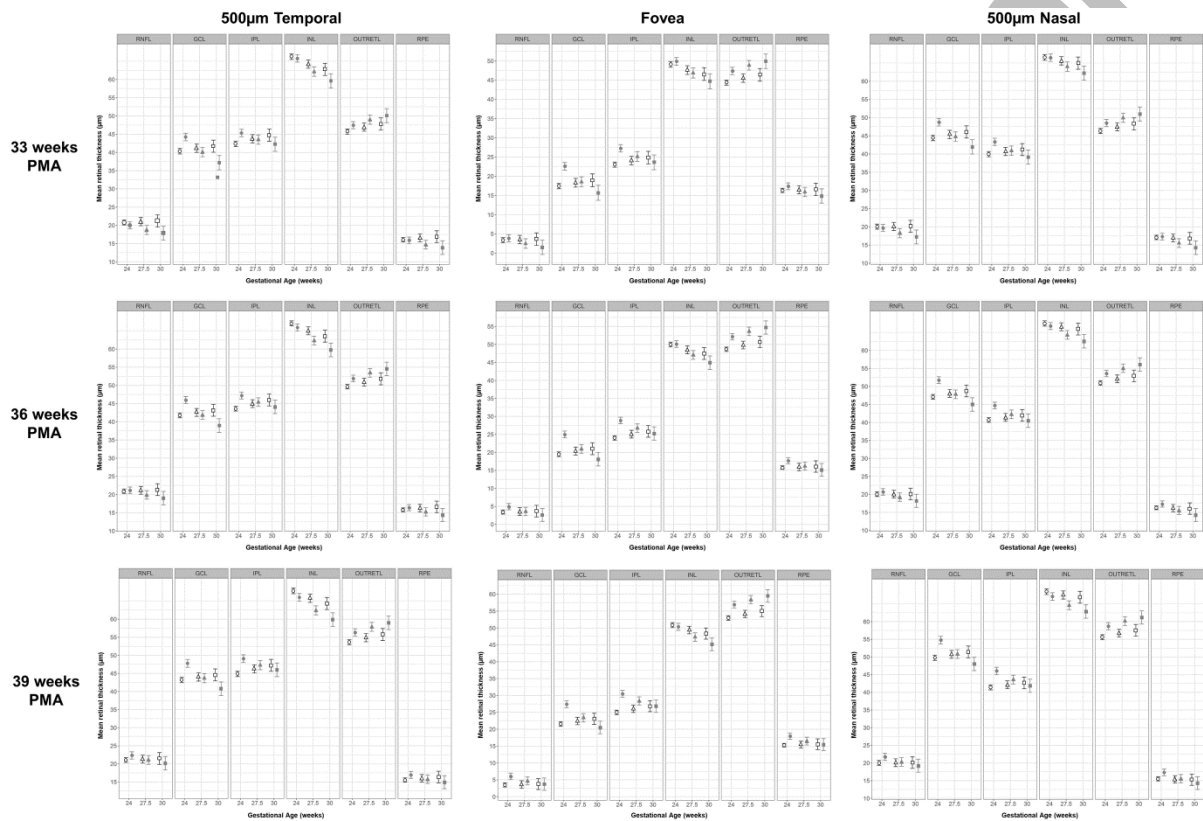


Differences are recorded at postmenstrual ages (PMA) of 33, 36 and 39 weeks where blue arrows indicate thinner layers in the ROP groups and red arrows that layers are thicker. An example of a segmented B-scan at each age is shown below.

RNFL – retinal nerve fibre layer, GCL – ganglion cell layer, IPL – inner plexiform layer, INL – inner nuclear layer, OUTRETL – outer retinal layers, RPE – retinal pigment epithelium.

HH-OCT – hand-held optical coherence tomography

Figure 2. Foveal and parafoveal layer changes between 500 μm nasal and temporal retina associated with retinopathy of prematurity (ROP, shaded grey) and non-ROP (unshaded) at 24-weeks (circles), 27.5-weeks (triangles) and 30-weeks (squares) gestational age (GA) for 33-, 36- and 39-weeks postmenstrual age (PMA). Results are shown with 95% confidence intervals.



SDC1 Methodology using hand-held spectral domain optical coherence tomography (HH SD-OCT).

SDC2 Video 1 mp4 Dynamic mean retinal thickness changes at mean GA (27.5 weeks) with PMA from 33 to 39 weeks between ROP and non-ROP infants for macular retinal layers

SDC 3. Table 5. The predicted mean difference in retinal thickness (μm) between presence and absence of retinopathy of prematurity for foveal and parafoveal retinal layers at gestational age: (A) 24, (B) 27.5, and (C) 30 weeks. Results are shown with 95% confidence intervals **using 33 weeks postmenstrual age (PMA)** at 5 locations (fovea 0, 1000 μm and 500 μm nasal and temporal to the fovea). RNFL – retinal nerve fibre layer, GCL – ganglion cell layer, IPL – inner plexiform layer, INL – inner nuclear layer, OUTRETL – outer retinal layers, RPE – retinal pigment epithelium, padj – adjusted p-value.

SDC 4 Table 6. The predicted mean difference in retinal thickness (μm) between presence and absence of retinopathy of prematurity for foveal and parafoveal retinal layers at gestational age: (A) 24, (B) 27.5, and (C) 30 weeks. Results are shown with 95% confidence intervals **using postmenstrual age of 36 weeks** at 5 locations (fovea 0, 1000 μm and 500 μm nasal and temporal to the fovea). RNFL – retinal nerve fibre layer, GCL – ganglion cell layer, IPL – inner plexiform layer, INL – inner nuclear layer, OUTRETL – outer retinal layers, RPE – retinal pigment epithelium, padj – adjusted p-value.

SDC 5 Table 7. The predicted mean difference in retinal thickness (μm) between presence and absence of retinopathy of prematurity for foveal and parafoveal retinal layers at gestational age: (A) 24, (B) 27.5, and (C) 30 weeks. Results are shown with 95% confidence intervals **using postmenstrual age of 39 weeks** at 5 locations (fovea 0, 1000 μm and 500 μm nasal and temporal to the fovea). RNFL – retinal nerve fibre layer, GCL – ganglion cell layer, IPL – inner plexiform layer, INL – inner nuclear layer, OUTRETL – outer retinal layers, RPE – retinal pigment epithelium, padj – adjusted p-value.

Table 1. Retinal layer borders and definitions used in the study

Retinal nerve fibre layer	RNFL	ILM border to RNFL/GCL junction
Ganglion cell layer	GCL	RNFL/GCL junction to GCL/IPL junction
Inner plexiform layer	IPL	GCL/IPL junction to IPL/INL junction
Inner nuclear layer	INL	IPL/INL junction to anterior OUTRETL border
Outer retinal layers	OUTRETL	Anterior OUTRETL border to anterior border of RPE
Retinal pigment epithelium	RPE	Anterior to posterior borders of the RPE

Table 2. Participant and image characteristics according to ROP

	Always had ROP	Never had ROP	Mixed (ROP or no ROP)
Number of children			
Total 87 (100%)	19 (22%)	57 (65%)	11 (13%)
Male	7	33	7
Female	12	24	4
Caucasian	9	29	4

Non-Caucasian	10	28	7
Single birth	14	52	9
Multiple birth	5	5	2
Mean (\pm SD) * GA, BW, PMA			
GA (weeks)	26.1 \pm 1.98	28.6 \pm 2.43	26.6 \pm 1.79
BW (grams)	807 \pm 170	1154 \pm 423	864 \pm 179
PMA (weeks)	36.5 \pm 2.63	36.1 \pm 2.45	36.0 \pm 3.18
Number of images			
Total 278 (100%)	73 (26%)	156 (55%)	49(18%)
stage 1	12	-	11
stage 2	57	-	17
stage 3	4	-	2
Right eye	40	73	12 ROP
			10 no ROP
Left eye	33	83	18 ROP
			9 no ROP

*Gestational age (GA), Birthweight (BW), postmenstrual age (PMA), retinopathy of prematurity (ROP)

Table 3. Summary statistics on preterm infants according to ethnicity, multiplicity of birth and sex. PMA = postmenstrual age, GA = gestational age, SD = standard deviation.

Ethnicity								
	PMA at Exam (weeks)			GA at Birth (weeks)			Birth Weight (grams)	
	Non- caucasian	Caucasian		Non- caucasian	Caucasian		Non- caucasian	Caucasian
<i>Total</i>	46	41		46	41		46	41
<i>minimum</i>	31.29	31.57		23.43	24.00		635	500
<i>maximum</i>	41.85	41.85		35.71	34.00		3540	1750
<i>mean</i>	35.73	36.25		27.84	28.59		1077	1091
<i>SD</i>	2.76	2.47		2.70	2.48		498	341
<i>median</i>	35.71	36.85		27.93	28.71		970	1100
<i>p value</i>	p=0.36			p=0.18			p=0.88	
Multiplicity of birth								
	PMA at Exam (weeks)			GA at Birth (weeks)			Birth Weight (grams)	
	single birth	multiple birth		single birth	multiple birth		single birth	multiple birth
<i>Total</i>	75	12		75	12		75	12
<i>minimum</i>	31.29	31.57		23.43	24.43		500	555
<i>maximum</i>	41.85	40.00		35.71	29.57		3540	1370
<i>mean</i>	35.99	35.86		28.32	27.42		1093	1020
<i>SD</i>	2.54	3.26		2.72	1.67		450	272
<i>median</i>	36.43	35.71		28.57	27.21		1042	1025

<i>p value</i>	p=0.89			p=0.13			p=0.45		
Sex									
	PMA at Exam			GA at Birth			Birth Weight		
		(weeks)			(weeks)			(grams)	
	All infants	Female	Male	All infants	Female	Male	All infants	Female	Male
<i>total</i>	87	40	47	87	40	47	87	40	47
<i>minimum</i>	31.00	31.57	31.29	23.43	23.43	24.29	500	555	500
<i>maximum</i>	43.85	39.57	41.85	35.71	34.71	35.71	3540	3540	2430
<i>mean</i>	36.20	35.63	36.36	28.19	27.84	28.49	1083	1038	1122
<i>SD</i>	2.64	2.33	2.85	2.61	2.73	2.49	429	510	347
<i>median</i>	36.00	35.78	36.71	28.43	28.29	28.71	1042	915	1120
<i>p value</i>		p=0.27			p=0.25			p=0.38	

Table 4. The predicted mean difference in retinal thickness (μm) between presence and absence of retinopathy of prematurity for foveal and parafoveal retinal layers at postmenstrual age: (A) 33, (B) 36, and (C) 39 weeks. Results are shown with 95% confidence intervals using mean gestational age 27.5 weeks at 5 locations (fovea 0, 1000 μm and 500 μm nasal and temporal to the fovea). RNFL – retinal nerve fibre layer, GCL – ganglion cell layer, IPL – inner plexiform layer, INL – inner nuclear layer, OUTRETL – outer retinal layers, RPE – retinal pigment epithelium, padj – adjusted p-value.

A. 33 weeks PMA			LOCATION		

Downloaded from https://journals.lww.com/retina by 51.161.134.10 on 11/07/2023

		nasal-1000µm	nasal-500µm	0µm	temporal-500µm	temporal-1000µm
RNFL	<i>padj</i>	<0.001	<0.001	0.33	<0.001	<0.001
	<i>Mean (95% CI)</i>	-2.73 (-3.61, -1.85)	-1.86 (-2.65, -1.08)	-1.02 (-1.8, -0.23)	-2.29 (-3.08, -1.5)	-3.00 (-3.88, -2.12)
GCL	<i>padj</i>	0.060	1.0	1.0	0.51	<0.001
	<i>Mean (95% CI)</i>	-1.47 (-2.4, -0.54)	-0.6 (-1.44, 0.24)	0.25 (-0.6, 1.09)	-1.03 (-1.87, -0.18)	-1.74 (-2.67, -0.81)
IPL	<i>padj</i>	1.0	1.0	0.37	1.0	1.0
	<i>Mean (95% CI)</i>	-0.66 (-1.58, 0.26)	0.21 (-0.62, 1.04)	1.05 (0.23, 1.88)	-0.22 (-1.05, 0.61)	-0.93 (-1.86, 0.00)
INL	<i>padj</i>	<0.001	0.005	1.0	<0.001	<0.001
	<i>Mean (95% CI)</i>	-2.48 (-3.41, -1.55)	-1.61 (-2.45, -0.77)	-0.77 (-1.61, 0.08)	-2.04 (-2.88, -1.2)	-2.75 (-3.68, -1.82)
OUTR	<i>padj</i>	<0.001	<0.001	<0.001	<0.001	0.090
	<i>Mean (95% CI)</i>	1.62 (0.73, 2.51)	2.49 (1.7, 3.28)	3.33 (2.54, 4.13)	2.06 (1.27, 2.85)	1.35 (0.46, 2.24)
RPE	<i>padj</i>	<0.001	0.008	1.0	<0.001	<0.001
	<i>Mean (95% CI)</i>	-2.27 (-3.12, -1.42)	-1.4 (-2.16, -0.65)	-0.56 (-1.31, 0.2)	-1.83 (-2.59, -1.07)	-2.54 (-3.4, -1.69)
B. 36 weeks PMA				<i>LOCATION</i>		
		nasal-1000µm	nasal-500µm	0µm	temporal-500µm	temporal-1000µm

RNFL	<i>padj</i>	<0.001	0.27	1.0	0.0025	<0.001
	<i>Mean</i> (95% CI)	-1.7 (-2.44, - 0.96)	-0.83 (-1.46, - 0.21)	0.01 (-0.61, 0.64)	-1.26 (-1.89, - 0.63)	-1.97 (-2.72, - 1.23)
GCL	<i>padj</i>	0.12	1.0	1.0	1.0	0.011
	<i>Mean</i> (95% CI)	-1.12 (-1.88, - 0.35)	-0.25 (-0.9, 0.4)	0.6 (-0.06, 1.25)	-0.68 (-1.33, - 0.02)	-1.39 (-2.16, - 0.62)
IPL	<i>padj</i>	1.0	0.34	<0.001	1.0	1.0
	<i>Mean</i> (95% CI)	-0.03 (-0.79, 0.73)	0.83 (0.19, 1.48)	1.68 (1.04, 2.33)	0.41 (-0.24, 1.05)	-0.31 (-1.07, 0.46)
INL	<i>padj</i>	<0.001	<0.001	<0.001	<0.001	<0.001
	<i>Mean</i> (95% CI)	-3.13 (-3.9, - 2.36)	-2.26 (-2.92, - 1.6)	-1.42 (-2.08, -0.75)	-2.69 (-3.35, - 2.04)	-3.4 (-4.17, - 2.63)
OUTR	<i>padj</i>	<0.001	<0.001	<0.001	<0.001	<0.001
	<i>Mean</i> (95% CI)	2.09 (1.33, 2.85)	2.96 (2.32, 3.6)	3.8 (3.16, 4.44)	2.53 (1.88, 3.17)	1.82 (1.06, 2.58)
RPE	<i>padj</i>	0.002	1.0	1.0	0.029	<0.001
	<i>Mean</i> (95% CI)	-1.47 (-2.2, - 0.74)	-0.6 (-1.21, 0.01)	0.24 (-0.37, 0.85)	-1.03 (-1.65, - 0.42)	-1.74 (-2.47, - 1.01)

C. 39 weeks PMA

LOCATION

		nasal-1000µm	nasal-500µm	0µm	temporal-500µm	temporal-1000µm
RNFL	<i>p</i> adj	1.0	1.0	0.15	1.0	0.79
	<i>Mean</i>	-0.67 (-1.5,	0.19 (-0.54,	1.04 (0.31,	-0.23 (-0.97,	-0.95 (-1.78, -
	<i>(95% CI)</i>	0.16)	0.93)	1.77)	0.5)	0.11)
GCL	<i>p</i> adj	1.0	1.0	0.57	1.0	0.64
	<i>Mean</i>	-0.77 (-1.65,	0.1 (-0.69,	0.95 (0.16,	-0.33 (-1.12,	-1.04 (-1.93, -
	<i>(95% CI)</i>	0.12)	0.89)	1.74)	0.46)	0.15)
IPL	<i>p</i> adj	1.0	0.007	<0.001	0.28	1.0
	<i>Mean</i>	0.59 (-0.28,	1.46 (0.69,	2.31 (1.53,	1.03 (0.25,	0.32 (-0.55,
	<i>(95% CI)</i>	1.46)	2.23)	3.08)	1.81)	1.19)
INL	<i>p</i> adj	<0.001	<0.001	<0.001	<0.001	<0.001
	<i>Mean</i>	-3.78 (-4.68, -	-2.92 (-3.72, -	-2.07 (-2.87, -	-3.34 (-4.15, -	-4.06 (-4.95, -
	<i>(95% CI)</i>	2.89)	2.11)	1.26)	2.54)	3.16)
OUTR	<i>p</i> adj	<0.001	<0.001	<0.001	<0.001	<0.001
	<i>Mean</i>		3.43 (2.64,	4.27 (3.49,		2.29 (1.40,
	<i>(95% CI)</i>	2.56 (1.68, 3.44)	4.21)	5.06)	3 (2.21, 3.78)	3.17)
RPE	<i>p</i> adj	1.0	1.0	0.12	1.0	0.70
	<i>Mean</i>	-0.67 (-1.48,	0.2 (-0.51,	1.04 (0.33,	-0.23 (-0.94,	-0.94 (-1.76, -
	<i>(95% CI)</i>	0.14)	0.91)	1.75)	0.48)	0.13)

Downloaded from https://journals.lww.com/retinaljournal by BhdMj5epPhkav1zeoun1tQIN4a4kLlHEZgshHd4XMI0 on 11/07/2023